Bulletin of the New Zealand Society for Earthquake Engineering, Vol. 59, No. 1, March 2026

SEISMIC PERFORMANCE OF PRECAST HOLLOW-CORE FLOORS: EXPERIMENTAL FINDINGS AND UPDATES TO C5

Frank Büker[1], Nicholas J. Brooke[2], Lucas S. Hogan[3], Kenneth J. Elwood[4], Des K. Bull[5] and Timothy J. Sullivan[6]

(Submitted *March 2025*; Reviewed *April 2025*; Accepted *May 2025*)

ABSTRACT

Precast, prestressed hollow-core floors are susceptible to earthquake-induced damage and collapse. While significant progress has been made in New Zealand in understanding and assessing their seismic behaviour, the 2016 Kaikōura earthquake and recent testing demonstrated several unexpected damage patterns. This paper presents experimental evidence and proposes modifications to assessment procedures to account for the detrimental effect of web cracking and the heightened damageability of hollow-core floor units that are seated at or on intermediate columns (so-called 'beta units'). The experimental investigation involved two full-scale super-assembly experiments on a two-bay by one-bay reinforced concrete moment frame structure with hollow-core floors. Results showed that web cracking can initiate at low inter-storey drifts (~0.5%) and become widespread as drifts increase. Beta units exhibited distinct damage patterns and higher vertical dislocations at lower drifts compared to other units. A comparison between the tested response and predictions from the 2018 version of the New Zealand Assessment Guidelines C5 demonstrated low accuracy in the positive moment failure assessment, particularly for beta units. A revised positive moment failure assessment is proposed to simplify the assessment and account for the damageability of beta units. Additionally, the experimental data showed that beam elongation predictions according to C5 (2018) are overly conservative within the elastic range, and a mechanics-based modification is proposed to enhance the accuracy of the assessment. The proposed assessment changes aim to improve the predictive accuracy and better indicate when seismic retrofitting is necessary.

https://doi.org/10.5459/bnzsee.1745

INTRODUCTION

Precast hollow-core floors became an integral part of New Zealand's construction industry since their introduction to the market during the late 1960s [1]. Between 1981 and 2003 their use was widespread, with over 1.5 million square metres of hollow-core flooring installed in the three major New Zealand centres of Auckland, Wellington, and Christchurch [2]. Despite their prevalence, design standards at the time (NZS3101:1982 A1-A4 [3] and NZS3101:1995 A1-A2 [4]) provided limited guidance on the seismic design and detailing of these floors [1]. Concerns about the seismic safety of the gravity load path of hollow-core floors arose after the collapses during the 1994 Northridge earthquake [5,6] and a super-assembly experiment at the University of Canterbury [7,8]. In response, research efforts focused on developing more robust hollow-core floor detailing [9-13] and improving the understanding of the likely performance of existing detailing [14-16]. This work led to substantial revisions to the design of buildings with hollow-core floors, with the adoption of new connection details in the design standards (NZS3101:1995–A3 [17] and NZS3101:2006–A1-A3 [18]).

From the limited but high-quality research, detailed assessment procedures for existing hollow-core floors were developed [19]. The release of the assessment guidelines by Fenwick et al. [19] was overshadowed by the 2010/2011 Canterbury earthquake sequence [20,21] and, hence, did not receive widespread application. It was not until the 2016 Kaikōura earthquake that concerns about hollow-core floors and other precast flooring types were reignited. The earthquake resulted in the collapse of double tee flooring units in the Statistics house [22] and widespread damage to hollow-core floors, with many instances of moderate to severe damage [23,24]. A revised version of the Fenwick et al. hollow-core assessment guidance based on observations from the 2016 Kaikōura earthquake was incorporated in an update for the seismic assessment guidelines C5, which is herein referred to as 'Assessment Guidelines C5' [25].

The empirical assessment procedures suggest that floor performance and failure correlate strongly with the inter-storey drift imposed on the surrounding structure. Inter-storey drift creates local deformation demands on the flooring units, which include relative floor-to-support rotations, pull-off movement due to beam elongation and vertical incompatibility displacement between the hollow-core unit and the adjacent frame or wall elements. Based on previous experimental work, three main failure modes (Figure 1) were identified in the Assessment Guidelines C5 [25]. The first failure mode is loss of support (LOS), where the hollow-core floor unseats from the provided seating ledge. Another key failure mode is negative moment failure (NMF), which can take place in floors with light non-ductile mesh reinforcing in the topping layer (e.g. cold-drawn 665 mesh) and strong continuity reinforcement (e.g. starter bars) between the support and the floor. In such a configuration, the flexural strength at the end of the continuity

[1] *Corresponding Author, Postdoctoral Research Fellow, University of British Columbia, Kelowna, Canada, frank-bueker@gmx.de*
[2] *Managing Director, Compusoft Engineering Ltd, Auckland (Member)*
[3] *Senior Lecturer, University of Auckland, Auckland (Member)*
[4] *Professor, University of Auckland, Auckland (Fellow)*
[5] *Adjunct Professor, University of Canterbury, Christchurch and Technical Director, Holmes NZ LP, Christchurch (Life Member)*
[6] *Professor, University of Canterbury, Christchurch (Member)*

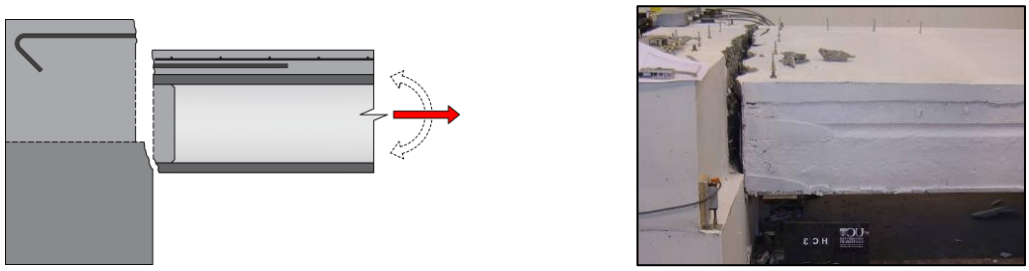

(a) Loss of support (Photo recorded by Jensen [15])

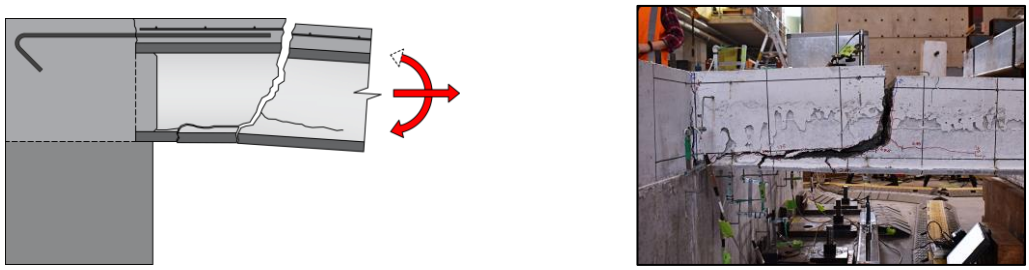

(b) Negative moment failure (Photo recorded by Büker [26])

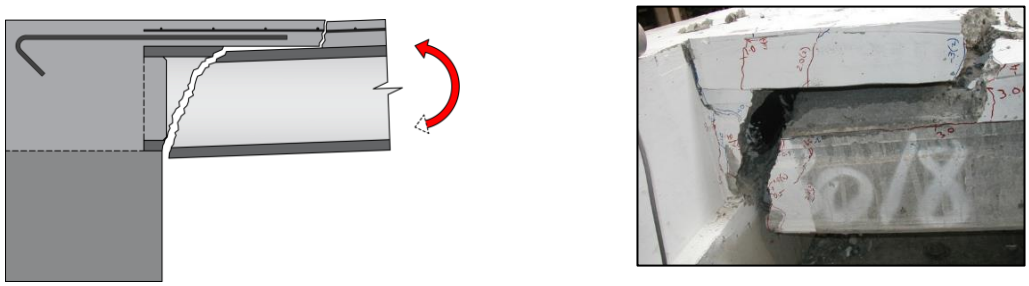

(c) Positive moment failure (Photo recorded by Bull and Matthews [9])

Figure 1: Main hollow-core floor failure modes (Arrows indicate actions that the floor connection depicted in the associated photo was subjected to. Red shading highlights the actions that caused the failure. Prestressing strands in the bottom of the floor are omitted for clarity.)

reinforcement suddenly drops, which may lead to a single negative moment crack in which deformations concentrate. The third failure mode, positive moment failure (PMF), arises when the hollow-core unit is tightly restrained between the top of the support beam and the topping slab, and rotation of the support beam relative to the floor causes a transverse flexural crack to form along the bottom face of the unit. For the general case, the 2018 version of the Assessment Guidelines C5 [25] consider a crack width equal to or larger than the strand diameter (typically 12.5 mm) as the limit of reliable support. A positive moment failure can also occur when there is a narrower positive moment crack and extensive web splitting, as observed by Matthews [8]. Such web splitting can be caused by the displacement incompatibility between the hollow-core floors and elements that are adjacent or parallel to the floor, such as beams or walls. These hollow-core units are commonly referred to as ‘alpha units’. Extensive torsional demands combined with a transverse soffit crack can also result in a positive moment failure.

The assessment procedures in the Assessment Guidelines C5 [25] do not estimate the drift at which the precast flooring unit collapses but rather estimate the drift at which gravity load paths become unreliable. For laboratory tests of precast floors, a vertical drop of 2 mm at the floor support has been used as a metric, indicating that gravity load paths have become unreliable [27]. Experimental evidence suggests there is some margin beyond this drift before actual collapse occurs, but the extent of this margin varies.

Figure 2: Soffit damage in a ‘beta unit’ recorded following the 2016 Kaikōura earthquake [29].

Several important damage observations from the 2016 Kaikōura earthquake remained unaccounted for in the Assessment Guidelines C5 [25]. Mostafa et al. [24] reported that hollow-core units supported on or close to intermediate columns were, in some instances, heavily damaged, while adjacent units remained largely undamaged (Figure 2). These hollow-core units have come to be referred to as ‘beta’ units and differ from alpha units in that there is no parallel beam or wall running adjacent to the hollow-core unit. Another key issue that was emphasised by observations from the 2016 Kaikōura earthquake and previous experiments was the susceptibility of hollow-core floors to cracking in the webs. Cracks in the webs

are particularly critical for hollow-core units because the webs of these extruded elements are unreinforced and rely on the uncracked capacity to resist shear. Several studies [23,24,28] suggested that the web cracking and beta unit concerns may not be appropriately addressed in the Assessment Guidelines C5 [25].

This paper investigates the behaviour of beta units and web cracks in hollow-core floors through experimental testing of two super-assembly specimens. Further, it proposes methods to account for these behaviours in the assessment. First, the methodology for the super-assembly testing is discussed, followed by a summary of the hollow-core floor performance and detailed discussions focused on web cracking and beta unit observations. Subsequently, the assessment procedures are evaluated against the observed experimental behaviour and improvements for the hollow-core floors assessment are proposed. Lastly, the beam elongation measurements from the super-assembly experiments are evaluated against the assessment guidelines and improvements to the pre-yielding range are proposed. Notably, this study focuses on the degradation of the gravity load path in hollow-core floors, while the in-plane diaphragm behaviour is beyond its scope.

TEST PROGRAMME

Two super-assembly test specimens were constructed and tested in the laboratory facilities at the University of Canterbury in Christchurch, New Zealand. These tests were conducted as part of the RECAST project [30] that led to a number of useful contributions relative to the seismic assessment and retrofit of reinforced concrete buildings with hollow-core floors [24,29,31–39]. This section provides relevant information on the test methodology for this paper, but for more details, readers are referred to Büker [26].

Each specimen consisted of a two-bay by one-bay reinforced concrete frame with precast hollow-core floor units (Figure 3a) and was a full-scale representation of a segment from a multi-story, moment-resisting frame building. Within the frame, eight 200 mm deep hollow-core units with 75 mm cast-in-place topping formed the floor plate. The hollow-core units were labelled U1-U8 from east to west, with U1 and U8 being alpha units and U4 and U5 being beta units. Each hollow-core unit spanned 7.1 m in the one-bay direction, which was a common floor configuration in buildings constructed in the 1980s in Wellington, New Zealand [40]. Another existing building feature was the eccentric positioning of the beam and column centrelines, which resulted in the columns protruding into the floor plate.

The support connection had starter bars lapping onto the 665 mesh in the topping layer, providing continuity between the frame and the floor diaphragm (Figure 3b). As-built seating lengths varied between 15 and 55 mm. The floor was placed directly against the adjacent parallel beams, with starter bars reaching from the top of the beam into the topping layer (Figure 3c).

The tested beta unit support configuration had the notched hollow-core unit end supported on the plastic hinge region of the beam, as illustrated in Figure 4. In this arrangement, the floor was not directly connected to or seated on the intermediate columns, but column ties provided some degree of continuity.

A simulated design of the frame was done to the 1984 New Zealand design standard (NZS4203:1984) [41] to arrive at member sizes and strength requirements representative of construction at the time, as described in De Francesco et al. [42]. The frame components were subsequently designed and detailed by Parr [43] to comply with the most recent ductile seismic design requirements as per NZS3101:2006-A3 [18]. Using the most recent design provisions for the reinforced concrete frame was desired to ensure that the floors could be tested to high inter-storey drift demands without premature frame failure. In both experiments, the frame performed in a ductile manner as per design, with plastic hinges forming in the reinforced concrete beams while the columns remained elastic.

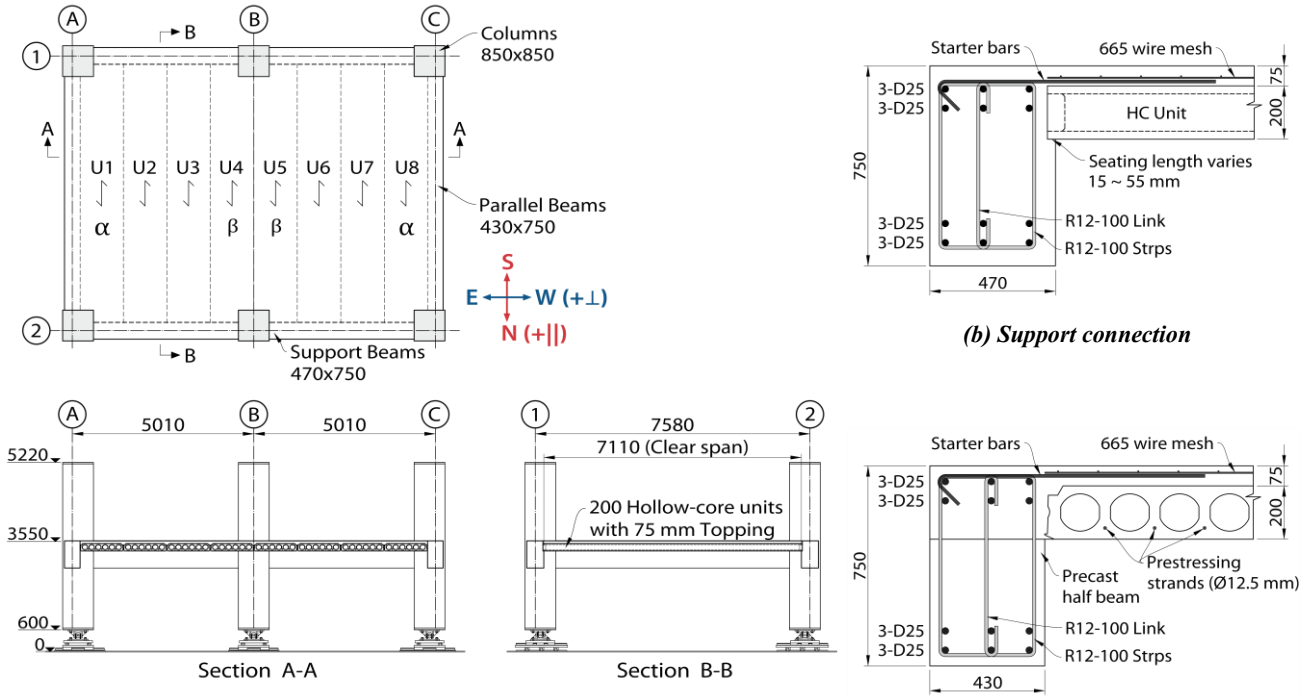

(a) General specimen configuration

(b) Support connection

(c) Connection to parallel beam

Figure 3: Super-assembly test specimen with nominal dimensions (modified from Büker et al. [39]).

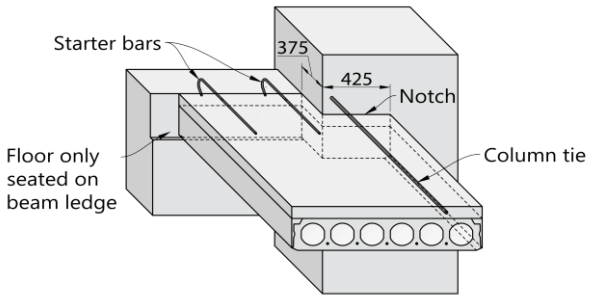

Figure 4: Beta unit detailing.

The detailing and performance of the floor in Test 1 is not discussed in this paper because the floor behaviour could not directly be compared to the assessment predictions due to the influence of retrofits, the premature completion of the experiment at 3% inter-storey drift and torsional softening of the beam plastic hinges (refer to Büker [26]). Test 2 featured varying starter bar configurations, as shown in Figure 5. Most notably, the configuration along support B1C1 was intentionally designed to be highly susceptible to NMF. A saw cut was made along the end of the starter bars along this support to replicate shrinkage cracking. The provision of the saw cut aligns with the premise of the assessment procedures because the concrete is assumed to be cracked in the NMF assessment in the Assessment Guidelines C5 [25]. Test 2 also incorporated post-installed column ties with transverse stitching bars, as indicated in Figure 5.

The setup for the super-assembly tests was designed to allow simultaneous bi-directional earthquake loading. Relative displacements were applied at the top and bottom of the columns to simulate inter-storey drift using fourteen hydraulic rams mounted along an L-shaped strong wall. A loading frame transferred inter-storey drift demands between the columns, maintaining their approximate parallel alignment while allowing the beams to elongate due to inelastic flexural deformations, thereby permitting the frame to freely dilate horizontally. Furthermore, each column rested on bi-directional sliders with universal hinge joints that enabled outward movement due to the dilation of the frame.

The loading protocol of Test 2 is summarised in Table 1. Bi-directional inter-storey drifts were applied via quasi-static loading in displacement control. For a clear differentiation of the loading direction, inter-story drifts applied in the direction parallel to the hollow-core unit span (North-South direction) are marked with a '(||)' symbol, and inter-story drift demands transverse to the unit span (East-West direction) are marked with a '(⊥)' symbol (refer to Figure 3a). The achieved inter-story drift ratios varied slightly from the targeted inter-storey drift ratios. In the remainder of the paper, the achieved inter-storey drift ratios are referenced and simply referred to as 'drift'. Test 2 was initiated with low-intensity test (LIT) to check instrumentation. Then, the specimen was subjected to drift demands in accordance with a near-fault ground motion from the 1994 Northridge earthquake (NEQ) at the Rinaldi Receiving station. The drift demands were based on the simplified simulated third-storey response of a 1980s moment-resisting frame structure with hollow-core floors [42]. This near-fault earthquake featured a velocity pulse that resulted in a large drift demand of approximately -2% in the (||) loading direction, with only limited drift demands imposed in the preceding cycles. As the testing undertaken is quasi-static in nature, the motion imposed does not include an actual velocity pulse, but the imposed drift demands are considered representative of those caused by an earthquake with a velocity pulse. Subsequently, a standard loading protocol with progressively increasing drifts (SLP) was performed in an elliptical bi-directional loading fashion. Intermittently, additional loading phases called Rhomboid (ROM) were executed through in-plane distortion of the diaphragm. These additional loading phases were carried out to capture the change in load paths and in-plane diaphragm stiffness as the floors degraded during earthquake loading. The results from the Rhomboid loading are presented by Parr et al. [35-36]. However, the Rhomboid loading has been excluded from the current study on the basis that these loading phases did not have any significant impact on the gravity load-carrying performance of the floors.

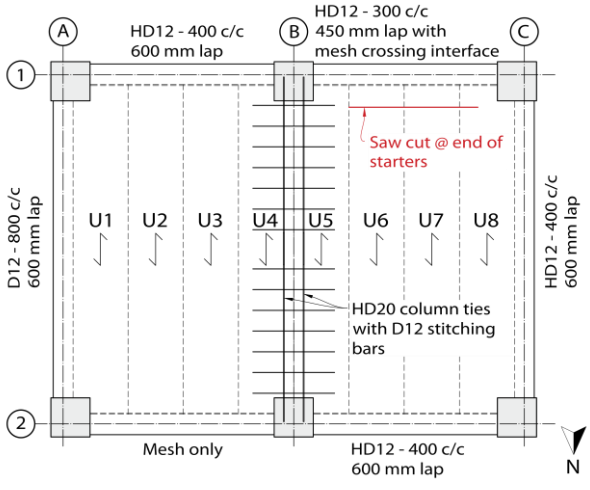

Figure 5: Configuration of Test 2.

The hollow-core floors also incorporated two different kinds of retrofits in the east and west bay [26,37,44]. The retrofit in the west bay (units U5-U8) was a strongback-type retrofit installed directly underneath the hollow-core units [37]. Due to some tolerances in the installation, the retrofits only started to engage with the hollow-core units at a vertical drop of approximately 1-3 mm. The floors in the east bay (units U1-U4) were retrofitted with a catch system incorporating structural cables. The cable catch retrofit first engaged with the hollow-core units in the east bay at a vertical drop of 10 mm. The damage observed at low-to-medium drift levels was not materially affected by the presence of the floor retrofits.

Table 1: Loading protocol and floor reinforcing of Test 2.

Loading Protocol						
Loading Phase	**No. of Cycles**	**Cycle**	**Targeted**		**Maximum Achieved**	
			(‖)	**(⊥)**	**(‖)**	**(⊥)**
LIT	2	1-2	0.125%	0.063%	0.109%	0.040%
NEQ	-	3	-2.0%	0%	-1.84%	0%
	-		+1.0%	0%	0.87%	0%
	-		0%	+1.0%	0%	0.84%
	-		0%	-1.0%	0%	-0.86%
SLP	-	ROM1			-	-
	1	4	1.5%	0.75%	1.42%	0.66%
	1	5	2.0%	1.0%	1.92%	0.89%
	-	ROM2			-	-
	1	6	2.5%	1.25%	2.40%	1.14%
	1	7	3.0%	1.5%	2.92%	1.37%
	-	ROM3			-	-
	1	8	3.5%	1.75%	3.44%	1.62%
	1	9	4.0%	2.0%	3.95%	1.88%
	-	ROM4			-	-
	1	10	0%	4.0%	0%	3.91%
	1	11	5.0%	2.5%	4.95%	2.45%

PERFORMANCE OF SUPER-ASSEMBLY EXPERIMENTS

The following discussion provides an overview of the floor performance observed in Test 2. For details of the behaviour and observations from Test 1, refer to [26,43]. The performance overview provided here has an emphasis on the internal floor damage and the vertical offset across soffit cracks (i.e. the vertical dislocation across a crack), as they are particularly relevant for the assessment comparison in the subsequent sections.

Overview of Damage Progression

The test commenced with a pulse to -1.84% (||) drift, which caused extensive damage to the floor units. At -0.31% (||) drift during the initial pulse, a negative moment crack formed within the saw-cut at the end of the starters along beam B1C1. This type of cracking was expected because the support connection was intentionally designed to be susceptible to negative moment failure.

The first web cracks were recorded with a borescope camera at -0.42% (||) drift at the north end of units U7 and U8 (Figure 6a). While these web cracks extended from the previously mentioned negative moment crack, the low drift at which they formed underscored the damageability of the unreinforced webs.

In addition, the first transverse cracking on the soffit of the hollow-core units occurred on the way to -0.42% (||) drift along the north support, with further soffit cracks forming while loading to -0.65% (||) drift. One of these transverse soffit cracks developed approximately 250 mm away from the support in alpha unit U1 (Figure 6b). This observation is significant because previous transverse soffit cracking in experiments formed close to the support (i.e., Figure 1c). Although this soffit crack only had a crack width of 0.3 mm, it extended internally as a diagonal web crack in the direction of the gravity shear toward the top of the floor.

At -0.87% (||) drift, the beta unit, U5, had dropped by 1.3 mm across the soffit crack at the north support. Following loading to -1.34% (||) drift, the vertical offset had doubled to 2.6 mm across the now 3 mm wide transverse soffit crack. This measurement surpassed the vertical offset benchmark of 2 mm, which is deemed to be an indicator of the loss of a reliable load path [27]. Even more substantial was the 3.7 mm vertical offset recorded across a soffit crack in beta unit U4 (north end). This transverse soffit crack formed about 100 mm from the seating ledge of the support beam and propagated internally as a shallow web crack over approximately 400 to 500 mm toward mid-span (Figure 6c).

As loading approached -1.84% (||) drift, the negative moment crack at the end of the starter bars along beam B1C1 continued to grow. From -1.44% (||) drift onwards, the 665 mesh at the end of the starter bars fractured, first at the corner column C1, then progressing to the middle column B1. At the peak of the initial push at -1.84% (||) drift, the negative moment crack had a width ranging from 3.5 mm (at beta unit U5) to 5.0 mm (at alpha unit U8) and a maximum vertical offset of 3.2 mm (beta unit U5).

Through inspection using borescopes, it was confirmed that there were web cracks in every hollow-core unit end at the peak of the first pulse (1.84% (||) drift). On the floor outside at the support ends, there were mostly transverse cracks visible on the top, bottom or both sides. Furthermore, an increase in vertical offsets across the transverse soffit cracks in beta units U4 and U5 was recorded, now measuring 6 mm and 4.5 mm, respectively. Figure 6d illustrates the extent of the vertical offset in beta unit U5. The retrofit installed under beta unit U5 was partially engaged at this point, whilst the retrofit type under beta unit U4 permitted further vertical dislocation.

(a) First web crack at the south end of unit U8 at -0.42% (||) drift.

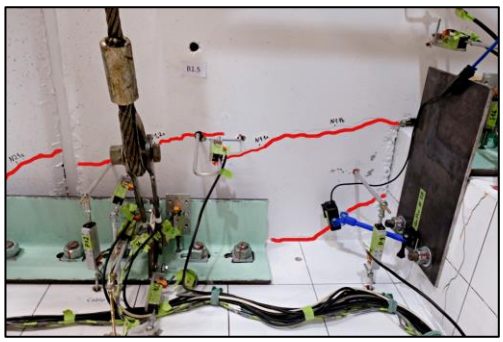

(b) Transverse crack in the north end of alpha unit U1 shown at -0.87% (||) drift.

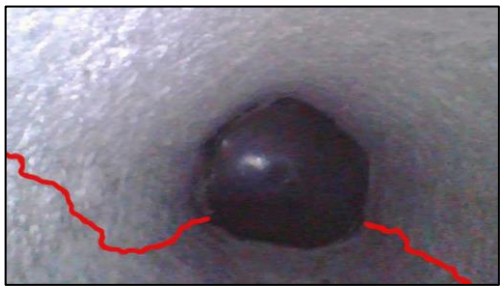

(c) Web cracking in beta unit U4 (North support) at -1.34% (||) drift.

(d) Vertical offset in soffit crack of beta unit U5 (North support) at -1.84% (||) drift.

Figure 6: Floor damage during NEQ Phase.

Significant additional damage to the hollow-core floor was observed during the standard loading protocol phase (SLP). At +1.51% (||) drift, the mesh at the floor-to-beam interface along support A2B2 ruptured during cycle 5. This support was detailed without starter bars and only relied on non-ductile 665 mesh that extended from the topping layer into the top of the beam. After the mesh fracture, the previously distributed negative moment cracking in the floor topping closed and deformations subsequently concentrated in the crack where the mesh fractured. The retrofits in the west bay started to partially engage during cycle 4 to 1.42% (||) but still let the floor undergo additional vertical offset subsequently.

As peak displacements increased, the web cracks expanded considerably, as illustrated in Figure 7a at -2.42% (||) drift. The gravity load paths in the hollow-core units at the support ends became severely compromised. Beta unit U4 experienced a substantial vertical drop of up to 25 mm at -2.92% (||) drift, while the alpha unit U1 only incurred a 10 mm vertical offset despite heavy damage in its support region. The smaller vertical offset in the alpha unit was likely due to load sharing between the adjacent beam A1-A2, alpha unit U1, and unit U2. Although this load path could not be considered structurally reliable, it evidently helped reduce the vertical drop of the alpha unit at this stage of the test. The retrofit underneath unit U2 engaged at the subsequent loading to +2.87% (||) drift.

While loading to -3.44% (||) drift in cycle 8, the mesh along beam A1B1 fractured in a topping crack running along the end of the starter bars. Following the mesh fracture, units U1-U4 experienced a vertical displacement of up to 40 mm. This damage also exaggerated the web cracking (Figure 7b). At this stage, all hollow-core floor units were at least partially supported by the retrofits installed underneath.

The test was continued until a peak drift of 4.95% to test the retrofit performance [26,44]. While a collapse was prevented by the retrofits, an incipient progressive collapse could be anticipated for an un-retrofitted hollow-core floor between 2% and 2.5% drift due to the extensive web cracking and the negative moment failure.

(a) Web cracking at the north end of unit U8 at -2.42% (||) drift.

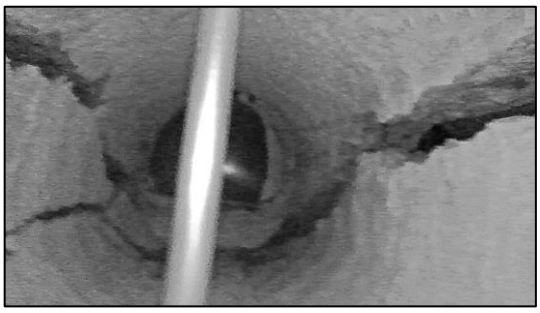

(a) Web cracking at the south end of beta unit U4 at +3.44% (||) drift.

Figure 7: Floor damage during the SLP Phase.

Web Cracking

As indicated in the damage progression summary above, earthquake loading can cause substantial cracking of the hollow-core webs. Such cracking is of particular significance because extruded hollow-core units lack vertical shear reinforcement. However, the design load path relies on the uncracked capacity of the prestressed concrete to resist the shear demands. In the super-assembly experiment, web cracking in the hollow-core floors substantially compromised the gravity load path. This was demonstrated through a gravity test of a hollow-core unit with moderate web cracking following Test 1, where the hollow-core unit could only sustain 54% of its un-factored design web shear cracking capacity [26].

Test 2 was particularly valuable in providing quantitative insights into the web crack development under loading conditions consistent with the Assessment Guidelines C5 [25]. Throughout the test, internal web damage was monitored using borescope cameras. A systematic review of the borescope photos indicated that the web cracks propagated at different slopes, with the web crack slope being defined as the inclination relative to the horizontal plane and denoted by angle α. Figure 8 shows examples of web cracks with (a) steeper and (b) shallower inclinations.

Shallower web cracks are deemed more detrimental to the gravity load-carrying capacity of the floor compared to steeper web cracks. A shallow web crack generally impairs a longer length of the floor, often running along the strand, which reduces the effectiveness of the strand to act in dowel action. In addition, a shallower angle lowers the contribution of aggregate interlock to resist vertical shear forces.

Due to the high degree of variability in the shape of the web cracks, a categorisation was conducted to generalise the dataset. Each borescope location was evaluated based on the following categories:

- Steep slope ($\alpha > 45°$)
- Moderate slope ($45° \geq \alpha > 22.5°$)
- Shallow slope ($\alpha \leq 22.5°$)
- No web cracking

The categorisation of the web cracks was conducted visually from the borescope photos as part of the data post-processing. Wherever multiple web cracks or a change in slope occurred, the shallowest part (when of significant length) was used for the categorisation.

Figure 9 illustrates the formation, progression and slope of web cracks with respect to borescope location and drift demand. Inspection locations are marked by circles, with shading indicating the crack angle category. Unit ends without a circle were not inspected with the borescope camera. The figure shows that the number of web cracks increased with higher drift demands. As the drifts increased, the web cracks tended to propagate at a shallower angle or additional shallow web cracks formed. The data for the figure only reflects the web cracks that were detectable in the borescope images. There may have been additional undetected web cracks that were initially missed and only detected at a higher drift level when crack widths were larger or not detected at all.

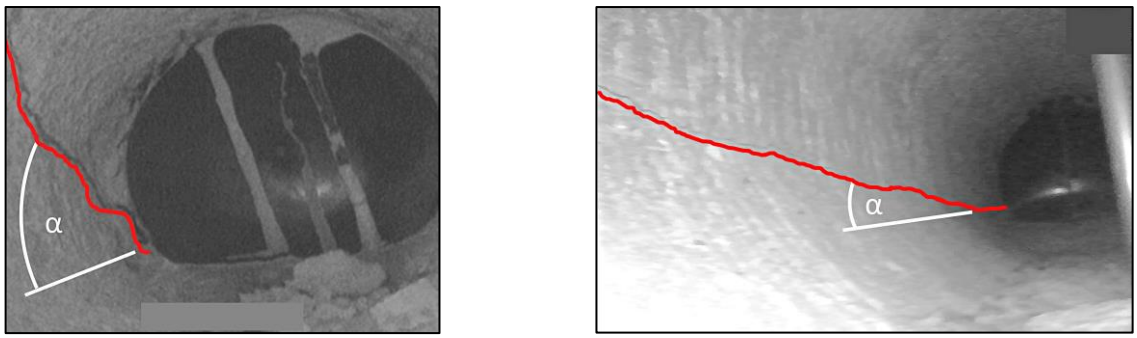

(a) Steeper crack (Alpha unit U8 south at 1.91% (||) in Test 1)

(b) Shallower crack (Beta unit U4 south at 1.38% (||) in Test 2)

Figure 8: Examples of web cracks demonstrating the different slopes the cracks propagated at (Reproduced from Büker et al. [45]).

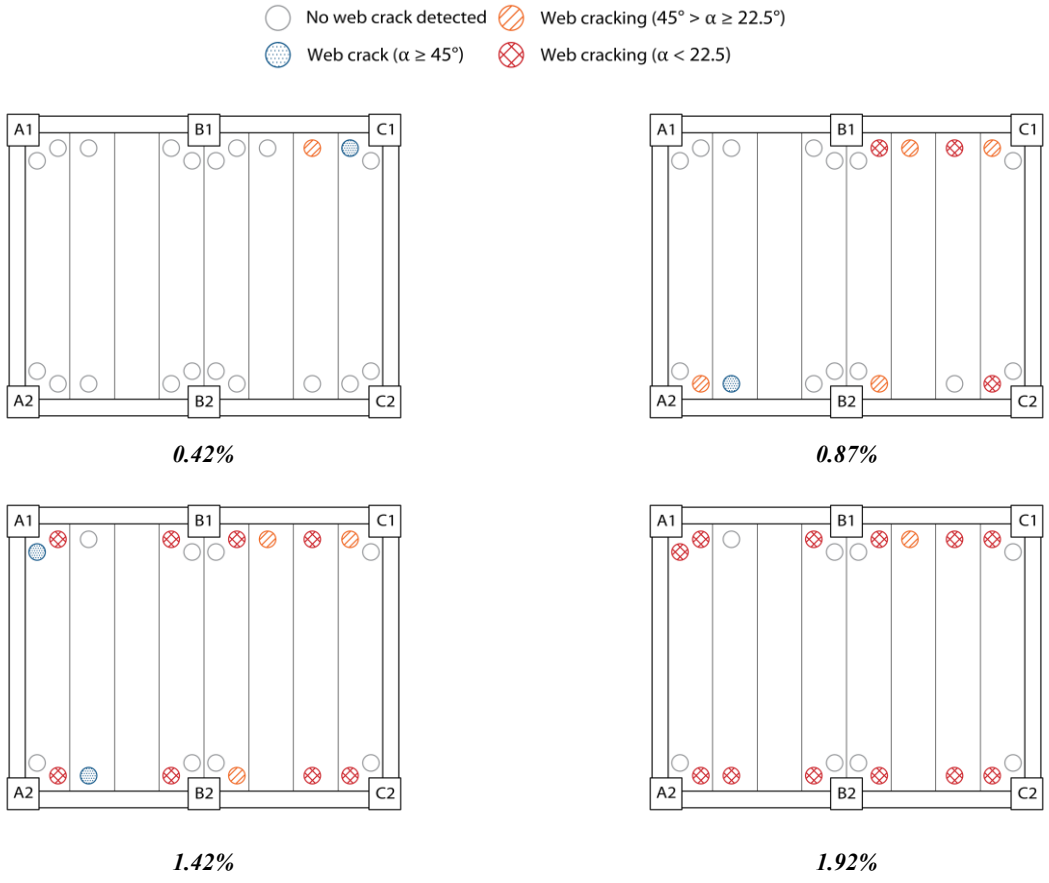

Figure 9: Location and slope of web cracking based on maximum (||) drift (Reproduced from Büker et al. [45]).

The bi-directional loading of the specimen provided insights into the influence of the loading directions on the web cracking. Several hollow-core units were equipped with displacement gauges to track the web crack width. Figure 10a shows the measured web crack width obtained from the instrument in beta unit U4 separated by loading direction. The web cracks formed during loading in the (||) direction. Further loading in the (||) direction led to widening of the web cracks, demonstrated by the increase in web crack width between the (||) peaks represented by the red dots. Similarly, (⊥) direction loading also resulted in widening of the web cracks, as indicated by the increased crack width between the (⊥) peaks (blue dots) for beta unit U4. However, web crack widening due to (⊥) loading was only observed in units supported on plastic hinges (i.e. alpha and beta units). A likely cause for this effect is the differential vertical displacements between the hollow-core unit and the support beam when undergoing negative rotations, as schematically illustrated in Figure 10b. With the sides of the flooring unit being vertically restrained by the parallel beam and adjacent unit, the floor end connection is pushed upwards as the support beam deforms due to negative rotations.

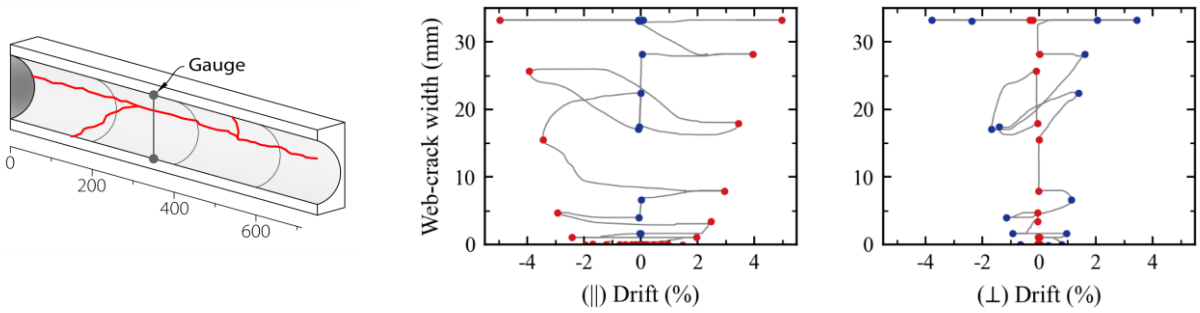

(a) Beta unit U4 South-East (Note that the instrument ran out of stroke at 33.2 mm web crack opening).

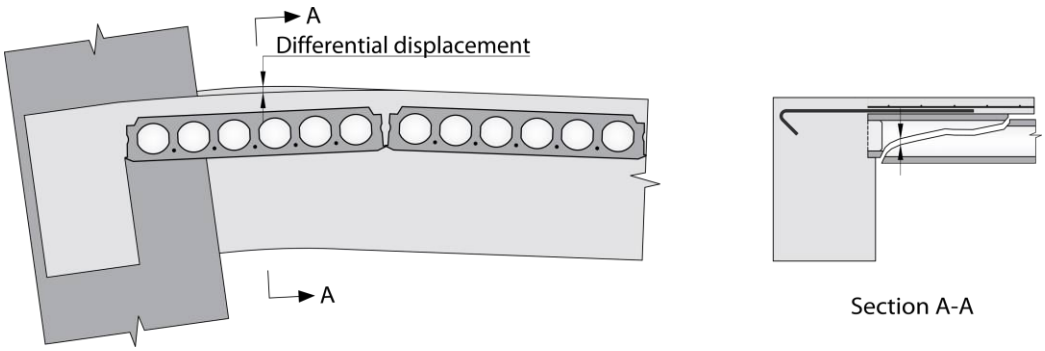

(b) Vertical differential displacement at the support induced by negative rotations of the support beam.

Figure 10: Effect of loading direction on web cracking.

Alpha and Beta Units

Both alpha and beta units tended to exhibit heightened concentrated damage at the supports, which raised concerns about the gravity load path. The vertical offset across soffit cracks can be taken as a quantitative indicator for the degradation of the gravity load path. In Figure 11, the vertical offset data was used to compare the degradation of the gravity load-carrying capacity for different hollow-core unit types (i.e., alpha, beta, and other units). As previously stated, a vertical offset of 2 mm was deemed to be an indicator of loss of reliable load path for hollow-core floor units [27]. In the super-assembly experiment, beta units clearly reached this benchmark at lower drifts than alpha units and other units.

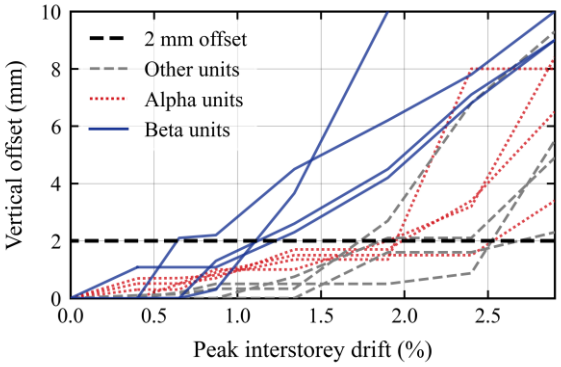

Figure 11: Vertical offset progression measured at the flooring unit ends (Note: The hollow-core unit types refer to alpha units (U1 and U8), beta units (U4 U5), and other units (U2-U3 and U6-U7)).

The damage in the tested beta units was extensive (Figure 12). The support region of these units incurred substantial transverse topping cracking up to 400 mm away from the support (Figure 12a). Such cracking away from the support is particularly unexpected for this support because it lacked starter bars and only comprised 665 mesh as continuity reinforcement. The predicted behaviour was the formation of a single crack along the cold joint at the floor-to-beam interface. The crack formation away from the support could be attributed to the discontinuity in the flooring unit created by the notches in the end region of the beta units around the inter-mediate columns (Figure 4). At the bottom of this hollow-core floor, the damage was concentrated in a single transverse crack 50 mm away at the seating ledge (Figure 12b). Internally, the top and bottom cracks joined via a shallow diagonal web crack (Figure 12c).

The web cracking was limited to the reduced floor section beside the notch. This section is particularly vulnerable due to its lower flexural and shear capacity as well as the limited prestress force within the transfer length of the strands. As indicated in the web crack drawings in Figure 12e, no internal damage was found in the webs along the width of the column. It should be noted that screw anchors (Figure 12d) were installed vertically through the hollow-core unit one meter away from the seating ledge as part of the cable catch retrofit. Borescope inspection indicated that these screw anchors helped to prevent the further propagation of the web cracks towards midspan of the floor.

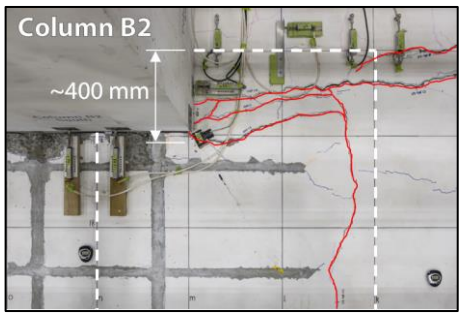

(a) Topping – dashed line indicating the perimeter of the flooring unit (+1.89% (||)).

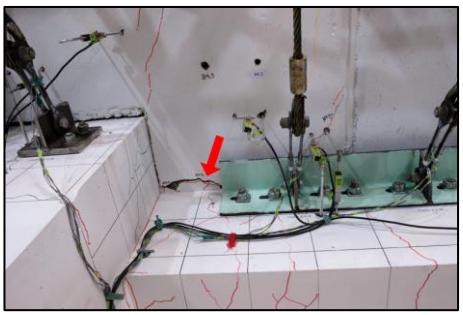

(b) Soffit (-1.92% (||)).

(c) Internal damage shown at residual after cycle 5 with -1.92% (||) peak drift (vertical element in the foreground is part of an instrumentation assembly.

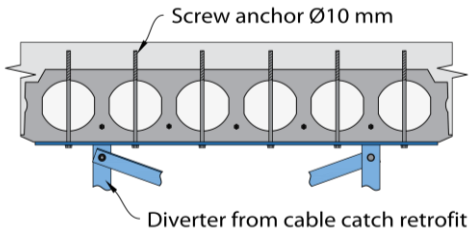

(d) Screw anchors.

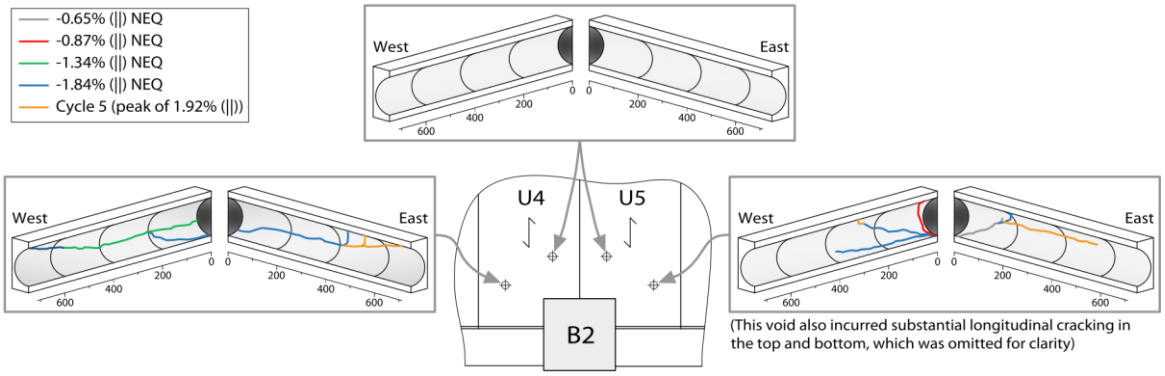

(d) Web cracking in beta units U4 and U5 at the north support. (Dimensions in millimetres).

Figure 12: Damage to beta unit U4 at the north support during cycle 5.

In contrast to the beta units, the alpha units exceeded the 2 mm vertical offset benchmark at a much later stage (Figure 11). One factor that limited the offset in the alpha units is the load sharing to the parallel beam adjacent to the alpha units. The cracking between the alpha unit and the parallel beam was limited, and therefore, it was likely that the gravity loads of the alpha units were partially carried by the parallel beam. In addition, some alpha unit support ends, particularly in unit U1, sustained distributed transverse soffit cracking during the experiment. The presence of several cracks allowed the unit to accommodate the vertical offset across several cracks. Since the vertical offset shown in Figure 11 is defined as the maximum vertical offset across each of the soffit cracks in a unit end, the accumulation of vertical offset across multiple cracks was not captured.

All web cracking in the alpha units occurred close to the end supports and was considerably less extensive compared to the damage in the alpha unit tested by Matthews [8]. Alpha units in the Matthews test sustained horizontal splitting in the webs (Figure 13a), which resulted in partial floor collapse of the alpha unit at 2.5% drift (Figure 13a). The splitting was due to the displacement incompatibilities between the alpha unit and the adjacent beam. Alpha units in the Matthews test spanned past an intermediate column and, therefore, had 4 locations along the length of the units where large relative vertical displacement demands were imposed (Figure 13c). In contrast, the alpha units in this new test did not span across an intermediate column and only had high relative displacement demands close to the support. In addition, hollow-core units that span multiple bays tend to span longer distances and require deeper units. In Matthews's case, the hollow-core units were 300 mm deep and had fewer more slender webs compared to the hollow-core units in the herein-described tests. Based on this evidence, it can be concluded that alpha units spanning multiple bays and past a vertical element tend to be more vulnerable to premature collapse.

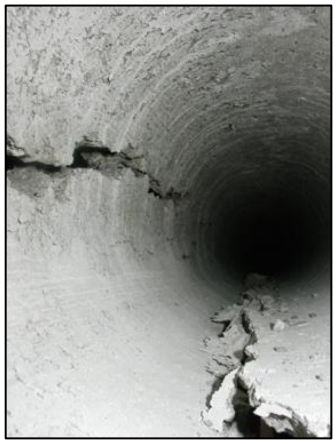

(a) Internal damage recorded at 2% drift [8].

(b) Collapse of the bottom part of the alpha unit at 2.5% drift [8].

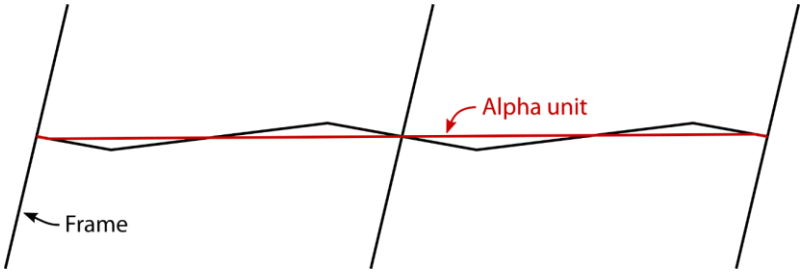

(c) Centre-line model of tested alpha unit configuration by Matthews [8].

Figure 13: Damage to the alpha unit in super-assembly test by Matthews [8].

COMPARISON OF ASSESSED TO MEASURED FLOOR PERFORMANCE

An important aspect of this study is the comparison of the super-assembly test performance against the assessment procedures in Appendix C5E of the Assessment Guidelines C5 [25]. A detailed seismic assessment of each hollow-core unit in the super-assembly specimens was conducted to determine the limiting drift capacity for the three failure modes. Table 2 summarises the assessed limiting drift alongside key experimental measurements as well as the observed failure mode. The assessment for LOS was conducted based on the as-built seating length without construction tolerance adjustments applied. In several cases, the as-built seating length was so short that the assessed drift capacity was 0% due to the consideration of initial spalling and lower bound elongation in the assessment. The failure in the ends of the units U2 and U3 were categorised as PMF-similar because the failure mechanism was mainly governed by the opening of a transverse soffit crack but ended up failing through mesh rupture in the topping.

Figure 14 plots the progression of vertical offset for the unit ends in the super-assembly test against the peak (||) drift. The figure incorporates the assessed drift capacities for the individual failure modes and highlights the 2 mm vertical offset benchmark with a dashed line. The failure mode, which led to the exceedance of the 2 mm vertical offset benchmark in the test specimen (i.e. the observed failure mode), is marked in red.

This visualisation indicates that in many cases, the drift at which the 2 mm offset is reached differs substantially from the assessed drift capacity of the observed failure mode. To further analyse this relationship, Figure 15a compares the assessed drift capacities for the observed failure mode with the measured drift capacities of the unit ends. For this purpose, the measured drift capacity is taken as the minimum of the drift at mesh fracture and the drift at which the 2 mm vertical offset benchmark was reached. It is important to note that the values for the assessed drift capacity in Figure 15a are based on the observed failure mode and not the minimum of the three failure modes.

The data suggests that the Assessment Guidelines C5 [25] assess the NMF capacity with relatively high accuracy. The 1% limiting drift for NMF appears to be appropriate for the tested frame specimen. Nonetheless, the PMF assessment shows relatively low accuracy in predicting the failure drift. In particular, the PMF capacities of unit ends U4S, U5S, U4N, U3N, and U6N are substantially over-predicted. On average, the capacity of those units is over-predicted by 133%, with the beta units (U4S, U5S and U4N) being the ones with the highest discrepancy. The commonality of these hollow-core unit ends is that they are all assessed to be located outside the zone that is affected by the elongation of the parallel beam (elongation zone). As such, the calculation of the PMF drift limits for units outside the elongation zone (i.e. U3 to U6) only takes into account the positive moment crack opening caused by the floor-to-support rotation demands and compares it to the PM crack limit taken as one strand diameter (typically 12.5 mm). The resulting assessed PMF capacity of 3.1% is non-conservative and does not agree with the observed performance in the test.

Figure 15b investigates the relationship between crack width and vertical offset for the flooring units that failed in PMF. It can be seen that at the point where the 2 mm vertical offset limit is exceeded, the positive moment crack width was less than 40% of the PMF benchmark crack width of 12.5 mm for all these unit ends. This comparison indicates that the 12.5 mm PMF crack width limit is not a reliable measure for the occurrence of PMF.

Table 2: Summary of the assessed capacity and observed key damage measurements. All values are reported in drift (Governing assessed drift capacity marked in bold).

Unit End	Assessed Drift Capacities			First Web Crack	Transverse/ Diagonal Soffit Crack Initiation****	Mesh Rupture	Drift w/ Vertical Offset ≥2 mm*****	Observed Failure Mode
	LOS**	NMF	PMF					
U1N	**1.1%**	Precluded	1.4%	-0.65% (||)	-0.65% (||)	+1.52% (||)	-1.92% (||) SLP	PMF
U2N	**0%**	Precluded	2.0%	-1.84% (||)	-0.65% (||)	+1.52% (||)	*No access***	PMF-similar
U3N	**0%**	Precluded	3.1%	*Not recorded*	-1.84% (||)	+1.52% (||)	*No access***	PMF-similar
U4N	**0%**	Precluded	3.1%	-1.34% (||)	-0.65% (||)	+1.52% (||)	-1.34% (||) NEQ	PMF
U5N	1.4%	**1.0%**	3.1%	-0.65% (||)	-0.65% (||)	–	-1.34% (||) NEQ*	PMF
U6N	1.4%	**1.0%**	3.1%	N/A	-0.87% (||)	–	-1.84% (||) NEQ*	PMF
U7N	1.4%	**1.0%**	2.0%	-1.34% (||)	-0.87% (||)	–	-2.92% (||) SLP*	PMF
U8N	**0%**	1.0%	1.4%	-0.87% (||)	-0.42% (||)	–	-2.92% (||) SLP*	PMF
U1S	1.3%	**1.0%**	1.4%	-1.34% (||)	-1.34% (||)	-3.44% (||)	-2.40% (||) SLP	PMF
U2S	1.8%	**1.0%**	2.0%	2.4% (Cyc 6)	N/A	-3.44% (||)	*No access***	PMF-similar
U3S	2.6%	**1.0%**	3.1%	*Not recorded*	+0.39% (||)	-3.44% (||)	*No access***	PMF-similar
U4S	2.2%	**1.0%**	3.1%	-0.87% (||)	+0.39% (||)	-3.44% (||)	+0.62% (||) NEQ	PMF
U5S	1.5%	**1.0%**	3.1%	-0.87% (||)	+0.15% (||)	-1.44% (||)	+1.38% (||) SLP*	NMF
U6S	1.2%	**1.0%**	3.1%	-0.65% (||)	+0.15% (||)	-1.44% (||)	+1.92% (||) SLP*	NMF
U7S	1.4%	**1.0%**	2.0%	-0.65% (||)	+0.15% (||)	-1.44% (||)	+2.87% (||) SLP*	NMF
U8S	1.8%	**1.0%**	1.4%	-0.65% (||)	+0.15% (||)	-1.44% (||)	-2.40% (||) SLP*	NMF

* Retrofitted with strongback retrofits, which may have reduced vertical offset.

** Based on the actual seating ledge provided.

*** Retrofit restricted access to obtain measurements of vertical offset.

**** Transverse crack was defined as a soffit crack that crosses two or more webs.

***** Reports the first inspection where the vertical offset in a soffit crack was ≥ 2 mm.

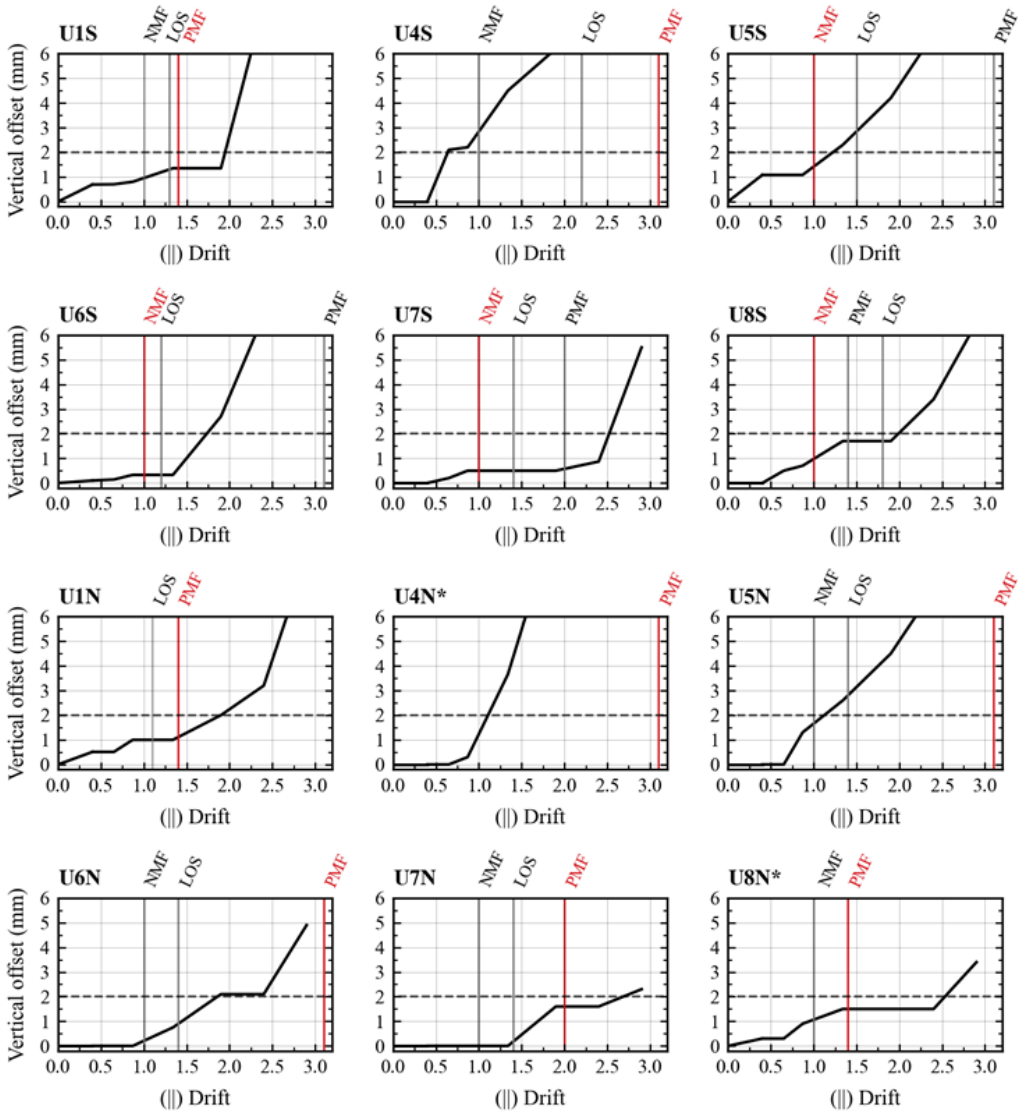

* *The assessed drift capacity for LOS is 0%.*

Figure 14: Vertical offset progression in Test 2 (Note: Red highlighting indicates the observed failure mode in the test).

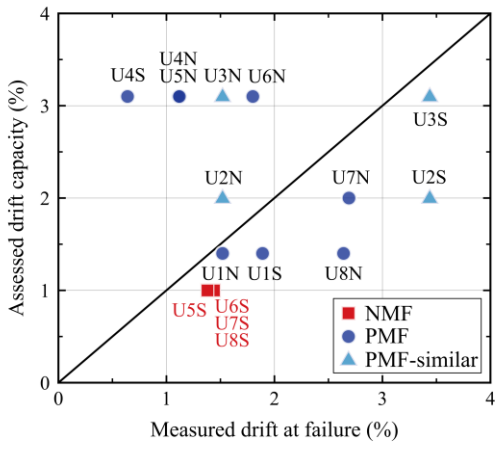

(a) Comparison of measured failure drift to assessed drift capacity based on the Assessment Guidelines C5 under consideration of the observed failure mode.

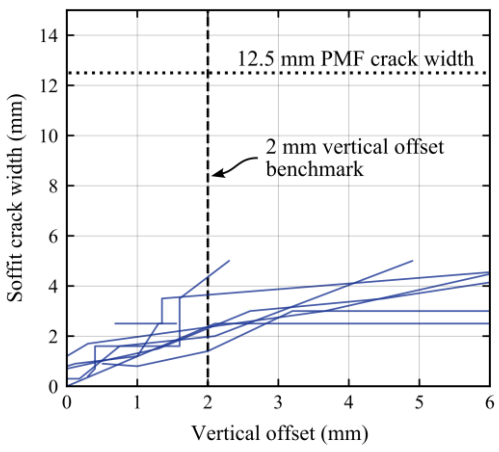

(b) Comparison of the vertical offset to crack width for the unit ends that failed in PMF [8].

Figure 15: Comparison of assessment to observed behaviour in Test 2.

The rapid growth of vertical offset relative to the narrow crack width may be related to the angle of the web crack that extends from the soffit crack. Figure 16 demonstrates the difference between cases with steeper cracks and shallower cracks. The centre of rotation (COR) for shallow cracks lies further away from the support than for steep cracks. As such, positive rotation demands predominantly result in crack widening for steep web cracks (Figure 16a), while rotation demands in floors with shallow cracks result in a response dominated by vertical offset (Figure 16b). The original PMF assessment procedure based on the crack width was based on specimens with steep cracks [19]. In Test 2, the crack angles of the positive moment cracks were observed to be relatively shallow (Figure 9), which explains the observations in Figure 15b and the poor performance of the PMF assessment procedure in the 2018 version of the Assessment Guidelines C5 [25].

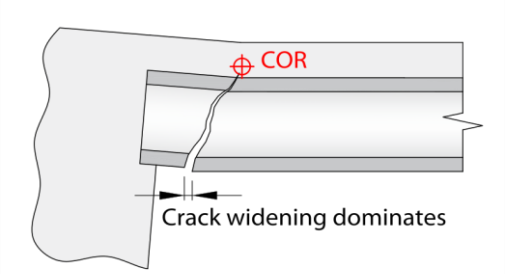

(a) Steep positive moment crack.

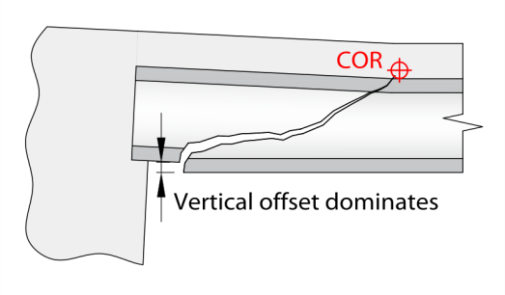

(b) Shallow positive moment crack.

Figure 16: Difference in centre of rotation (COR) for positive moment cracks at steep and shallow crack angles.

The previous discussion focused on comparing the observed drift at failure to the assessed drift capacity for the observed mode of failure. In practice, the floor performance is typically assumed to be governed by the failure mode with the lowest assessed drift capacities. Therefore, it is instructive to investigate the observed failure drift relative to the minimum assessed drift capacities considering all three failure modes, as shown in Figure 17. This plot shows that 15 out of the 16 tested hollow-core unit ends are assessed conservatively. While the NMF cases still show a relatively close correlation with the 1% drift limit, the floors that failed in PMF typically show high conservatism, which can be attributed to the following two factors:

1. LOS provides lower drift capacities than PMF, but LOS did not occur. The occurrence of either failure is dependent on where the dominant crack forms, i.e. at the floor-to-beam interface for LOS or in the soffit of the hollow-core unit close to the support for PMF. Because the cracks occurred within the hollow-core unit, the formation of LOS was unlikely. In addition, four hollow-core unit ends (U2N-U4N and U8N) had seating lengths shorter than 23.8 mm. For such short seating lengths, the assessed LOS capacity is 0%. This is because the available seating was shorter than the initial spalling, minimum bearing, and minimum elongation requirements in the assessment procedures. In response, this paper proposes improvements to the elongation estimates at low drift demands in one of the latter sections.
2. The unit ends at supports A1B1 (U1S-U4S) and B2C2 (U5N-U8N) were assessed to be susceptible to NMF but were only on the verge of meeting this criterion. While not failing in NMF during the experiment, the units had an assigned drift capacity of 1% for NMF. Given the severity of an NMF, the assessment incorporates some conservatism (e.g. considering the overstrength of continuity reinforcement, neglecting the uncracked capacity of the floor), which may lead to an assessment finding a floor vulnerable to NMF while not actually failing in negative moment during earthquake shaking.

These findings have critical ramifications for the assessment and retrofitting of hollow-core floors. In the latest retrofit design recommendations, Brooke et al. [32] suggest that retrofits should be designed following a failure-mode targeted approach (i.e. only the installation of retrofits that address the failure modes that the floor is assessed to be vulnerable to are required). Under consideration of this retrofitting approach, there are two key implications from the above findings. Firstly, the conservatism in the assessment (Figure 17) increases the retrofit needs, leading to higher costs and making retrofitting the floor a less attractive option. However, as previously noted, the occurrence of a particular failure mode depends on the type and location of cracking, which cannot be predicted given the current knowledge.

Secondly, the PMF assessment has been shown to be significantly unconservative for floors outside the elongation zone, and in particular, beta units. In real structures with exterior moment-resisting frames, the majority of the hollow-core units are located outside the elongation zone [26,29]. The unconservative PMF assessment means that many of these critical units may remain un-retrofitted for PMF in practice.

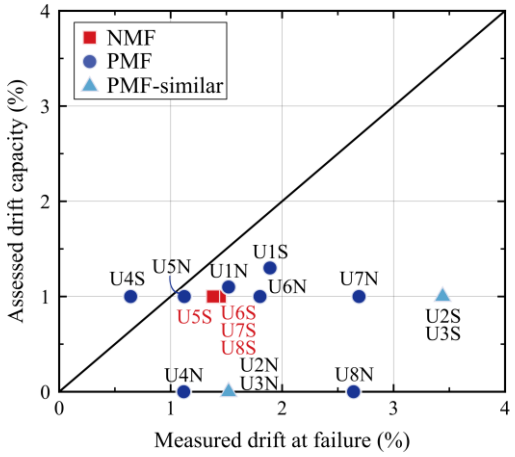

Figure 17: Comparison of measured failure drift to minimum assessed drift capacity based on the Assessment Guidelines C5 under consideration of all failure modes.

PROPOSED PMF ASSESSMENT PROCEDURE

In response to these findings, a new PMF assessment procedure has been proposed (Table 3). In recognition of the uncertainty in the hollow-core floor crack propagation, the procedure removes the implied precision of calculating the PMF capacity based on crack width, incompatibility displacement or torsional deformations. Instead, the proposed provisions introduce evidence-informed drift limits that are deemed suitable for different types of hollow-core units, categorised in terms of their susceptibility of web cracking and positive moment damage that could compromise a reliable gravity load path. The four categories are defined based on the location of the hollow-core units in the floor layout and their detailing. The simplification of the assessment process also enhances consistency across assessments performed by different engineers by removing room for interpretations.

The procedure introduces beta units to the positive moment assessment, assigning them the same drift limit as alpha units spanning over one bay and hollow-core units subjected to high torsion (Category 2). Alpha units spanning over multiple bays (e.g. Matthews [8]) are recognised as highly susceptible to horizontal splitting and are, therefore, ascribed a lower drift limit (Category 1). Hollow-core units that are not alpha units, beta units or hollow-core units subjected to high torsion fall into the last two categories. The difference between categories 3 and 4 is the presence of a low-friction bearing strip or detailing based on Clause 18.6.7 of NZS 3101:2006-A3 [18]. If a bearing strip was used at the end support, the formation of a positive moment crack is deemed unlikely.

This new procedure not only simplifies the PMF assessment but also improves the accuracy of the assessment. Figure 18 compares the experimental PMF drift to the proposed PMF assessment procedure (Table 3). In addition to the relevant hollow-core units of Test 2, the data from other experiments in which positive moment failure occurred were incorporated, i.e. PMF1 [9] and PMF3 [46], as identified by Corney et al. [27]. Experimental data exists for Category 2 (median of 1.32% drift and a standard deviation of 0.71% drift), Category 3 (median of 2.25% drift and a standard deviation of 0.96% drift) and Category 4 (No PMF observed). The absence of PMF in tested floors corresponding to Category 4 [10-13] confirms that PMF is very unlikely under these conditions. For some cases in Category 2 and 3 (e.g., PMF3 and U4S) the capacity is overpredicted. This overprediction is deemed acceptable as the 2 mm vertical offset used to determine the measured capacity is considered an indicator of loss of reliable load path and includes a margin toward collapse. No conclusive experimental data

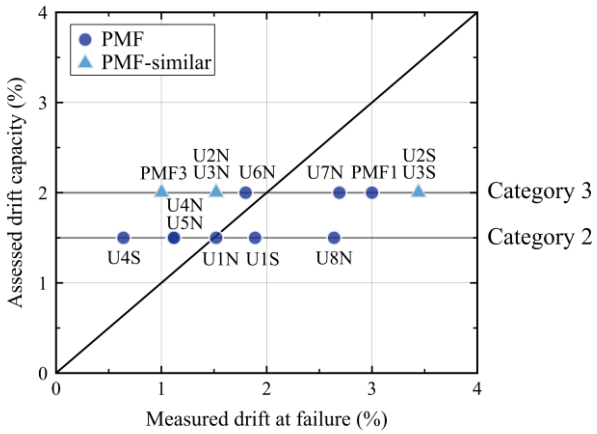

Figure 18: Comparison of measured failure drift to assessed drift capacity based on the proposed PMF assessment procedure presented in Table 3.

exist to evaluate Category 1 and the high torsion case in Category 2. The Matthews experiment [8] incorporated an alpha unit of Category 1 but there was insufficient vertical offset data to determine at what drift the 2 mm vertical offset was exceeded. The web splitting in the alpha unit was only detected at 2.5% drift when the web crack was already 25 mm wide.

While the proposed PMF assessment increases the accuracy of the PMF prediction, it does not improve the prediction of the governing failure mode for the super-assembly experiment presented in this paper. Even with the refined PMF model (Table 3), the assessment continues to predict the lowest drift capacity for LOS or NMF in the cases where a PMF failure was observed in the test. This is not unexpected because the occurrence of a given failure mode depends on where the cracks form and where the displacements concentrate. For instance, if no transverse cracks had formed in the soffit of the flooring units in the test, the floor had likely failed via LOS or an NMF. The uncertainty of crack location is recognised by Fenwick et al. [19] and the Assessment Guidelines C5 [25]. Nonetheless, the assessment and retrofit do not depend on determining the correct governing failure mode because each failure mode gets assigned a separate drift capacity in the assessment. The retrofit needs to address all the failure modes for which the assessed drift demand exceeds the assessed drift limits.

Table 3: Proposed drift capacities (considering median values) for the assessment of positive moment failure.

Category	Description	Potential for Web Cracking	Drift Limit
1	• Alpha units that span past a vertical element or system, for example, intermediate columns, walls, or braced frames.	High	1%
2	• Other alpha units • Beta unit • Other units subject to high torsion*	Moderate	1.5%
3	• Units that are not in Category 1, 2 or 4.	Low	2%
4	• Units that have either a low-friction bearing strip or detailing specified in Clause 18.6.7 of NZS 3101:2006-A3.	Limited	No limit

* Torsion should be considered in cases with significant relative twist between the two support ends of the unit (e.g., one end of the floor supported on a cantilever, coupling beam, link of an eccentrically-braced frame, wall or other elements that induce a high torsional twist).

BEAM ELONGATION MODEL REFINEMENT

The LOS assessment has a strong dependence on the elongation demands. As indicated in Table 2, the LOS assessment appears overly conservative for shorter seating length, which is primarily due to the lower bound elongation assumption of 0.5% of the beam depth. Enhancing the accuracy of the elongation model in the low-drift range is particularly relevant for determining whether a LOS retrofit is required in stiffer structures, upper storeys of a flexible moment frame or structures that are being retrofitted through adding lateral stiffness.

Beam elongation refers to the axial lengthening of a beam plastic hinge at the mid-height of the member. Fenwick and Megget [47] found that reversing plastic hinging leads to cumulative beam elongation with increasing deformation demands. This elongation significantly impacts the seismic performance of precast concrete floors because the lengthening of a beam parallel to the floor span can push the support beam away from the floor. This mechanism can lead to LOS or promote other non-ductile failures, especially when the beam elongation accumulates over multiple beam hinges, as demonstrated by the precast double-tee floor collapse in the 2016 Kaikōura earthquake [22,23].

The Assessment Guidelines C5 [25] recommend estimating the axial elongation of a reversing plastic hinge in a beam using the model in Equation (1). This equation is similar to the equation adopted for design in NZS3101:2006-A3 [18], with the difference of using plastic rotation, θ_p, as opposed to the total rotation, θ_m. Marder [48] showed that elongation predictions based on the plastic rotation, θ_p, provide a better match while using the total rotation, θ_m, is conservative and suitable for the design of new structures.

$$\delta_{el,rev} = 2.6\frac{\theta_p}{2}(d-d') \quad \begin{matrix} \leq 0.036h_b \\ \geq 0.005h_b \end{matrix} \tag{1}$$

where θ_p is the plastic rotation in the plastic hinge, d is the distance from the extreme compression fibre to the centroid of the tension reinforcement, d' is the distance from the extreme compression fibre to the centroid of the compression reinforcement and h_b is the beam depth of the gross section.

Equation (1) also includes an upper and lower bound elongation limit of 3.6% and 0.5% of the beam depth, respectively. The lower bound limit was introduced to conservatively account for the beam lengthening under elastic rotations [25]. This beam lengthening results from the neutral axis shift from mid-height of the beam toward the outer compression fibre once flexural cracks form.

Figure 19 compares the measured beam elongation of the south half of beam A1A2 to the elongation predictions defined in Equations (1). The measured elongation in Test 1 closely correlates with the predicted elongation (Figure 19a). The comparison also shows that the lower elongation limit of 0.5% of the beam depth significantly overestimates the elongation for the smaller drift cycles (i.e. <1.0% (||) drift). The elongation during these smaller drifts showed a gradual increase in elongation, which is not adequately reflected by using a constant lower bound.

Test 2 commenced with a unidirectional push to -1.84% (||) and, hence, lacked the accumulation of elongation through cyclic loading (Figure 19b). This first pulse, therefore, could rather be thought of as representative of the performance of a hinge under unidirectional loading. The model for a unidirectional plastic hinge, defined in Equation (2), appears more appropriate for the initial pulse. Using the plastic rotation, θ_p, as suggested in the Assessment Guidelines C5 [25] in Equation (2) under-predicts the elongation demands whilst using the total rotation, θ_p, as per NZS3101:2006-A3, slightly overpredicts the elongation during the pulse.

$$\delta_{el,uni} = \frac{\theta}{2}(d-d') \tag{2}$$

where θ is the beam rotation and can be substituted by the plastic rotation, θ_p or the total rotation, θ_m , and all other parameters have been defined previously.

Following this first pulse, the loading resumed in a reversing cyclic nature. In the remainder of the test, the measured elongation remained shy of the predicted elongation for reversing plastic hinges, particularly for loading in the negative direction. This effect may be attributed to the following aspects:

- The initial pulse to -1.84% (||) caused the plastic hinge to behave like a unidirectional plastic hinge, therefore resulting in smaller initial elongation and,
- Fewer cycles for a given drift level were applied in Test 2 compared to Test 1.

It should also be noted that the measured elongation exceeded the upper bound limit. As demonstrated by Büker [26], an exceedance of the upper limit was also observed in other tests [49].

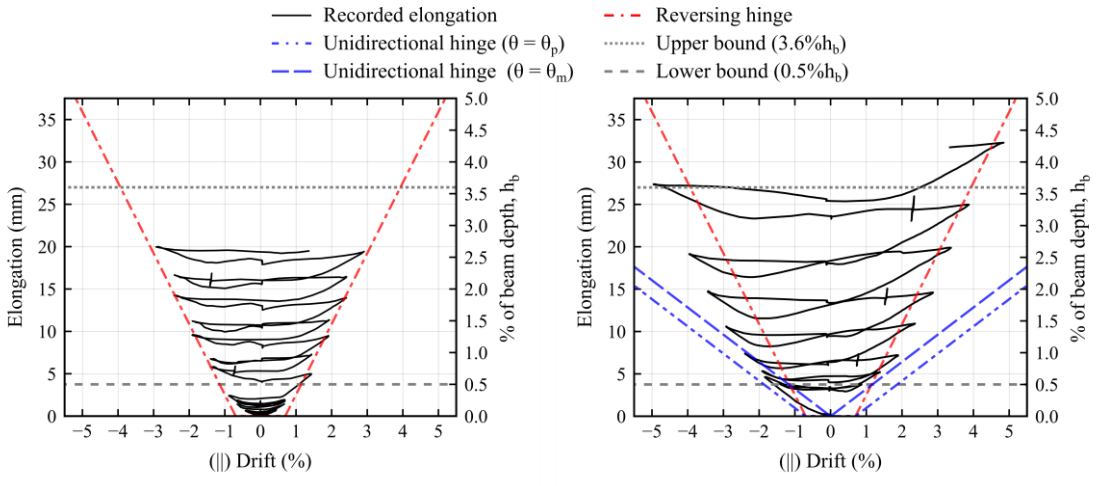

(a) Test 1 *(b) Test 1*

Figure 19: Elongation of beam A1A2 measured from column A1 to the midspan of the beam.

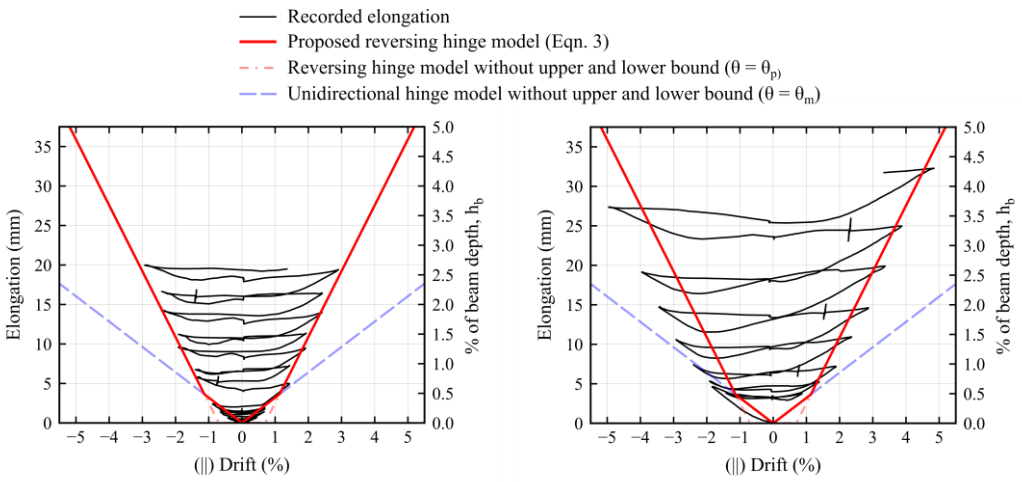

Figure 20: Elongation of beam A1A2 measured from column A1 to the midspan of the beam.

The data from the super-assembly tests showed that the lower bound of 0.5% of the beam depth overpredicts the elongation at low drift demands. A refined approach to determine the beam elongation at these low drifts would improve the assessment of hollow-core units. Therefore, this study proposes an alternative approach that replaces the lower bound elongation limit ($0.5\%h_b$) with the elongation of a unidirectional plastic hinge, $\delta_{el,uni}$, under consideration of the total elongation, θ_m, defined in Equation (2). The use of the unidirectional elongation prediction for low drift demands has a mechanics-based rationale. At these low drifts, the beams undergo axial elongation due to the movement of the neutral axis. The unidirectional elongation prediction equation approximates this shift geometrically.

Incorporating the unidirectional plastic hinge elongation as a lower limit yields Equation (3). In the absence of a reliable method to determine whether a beam has an upper limit of elongation, the upper bound elongation limit was not considered in this equation.

$$\delta_{el,rev} = \max\left(\begin{matrix} 2.6\dfrac{\theta_p}{2}(d-d') \\ \dfrac{\theta_m}{2}(d-d') \end{matrix}\right) \quad (3)$$

where all parameters have been defined previously.

Figure 20 demonstrates that the modified elongation model (Equation (3)) performs well at predicting the initial elongation for the hinge in Test 1. Although the model still overpredicts the elongation in Test 2, it represents an improvement over the constant lower bound elongation in the elastic range. Since no LOS failure was observed in the super-assembly experiment, the effect of the improved elongation model on the LOS prediction accuracy could not be evaluated, but future validation through testing or post-earthquake field investigation is recommended.

CONCLUSIONS

This paper presents proposed assessment improvements for the 2018 version of the Assessment Guidelines C5 [25] based on experimental data recorded during two super-assembly experiments. The first improvement targets the PMF assessment of hollow-core floors and the second is related to the beam elongation prediction within the elastic range. The main conclusions from the work discussed in this paper are as follows:

- Hollow-core floors are highly vulnerable to sustaining cracks in unreinforced webs under seismic deformation demands. These web cracks can occur at low drifts (0.4-0.5% drift) and typically propagate from transverse cracks that form in the soffit or the topping of the floor within the support region. The angle at which these cracks propagate can vary. In this test, the web cracks tended to get shallower as the drift demands increased. The number of hollow-core units affected increased with rising drift demands.
- Hollow-core units seated at the intermediate columns ('beta units') are more susceptible to damage than those supported closer to the mid-span of the support beam. The beta units were shown to be prone to extensive and shallow web cracking and flexural cracking away from the support promoted in part by notches cut out of the units.
- The Assessment Guidelines C5 [25] are generally conservative in assessing the overall limiting drift capacity (including all failure modes) of the tested hollow-core units.
- The assessment procedures for PMF are inaccurate at predicting the failure drift. For hollow-core units located outside the elongation zone, the prediction tends to be unconservative, overpredicting the PMF drift capacity by 133% on average in the experiment. In contrast, the drifts at NMF tends to closely align with the predictions by the Assessment Guidelines C5 [25].
- A new PMF assessment procedure is proposed that not only simplifies the assessment but also provides more accurate estimates of the expected (median) performance. This procedure also takes into account the heightened damageability of beta units not previously captured by the Assessment Guidelines C5 [25].
- Beam elongation predictions in the Assessment Guidelines C5 [25] were shown to over and under-estimate measured values for low and high storey drift demands, respectively. A refinement of the elongation model is proposed by replacing the current lower bound elongation of 0.5% of the beam depth with the elongation model for unidirectional plastic hinges, considering the total elongation demands. With the proposed changes, it is anticipated that fewer retrofits will be required in stiff buildings.

- The models proposed here have been implemented in the recently released 2025 update to the Assessment guidelines C5 [50].

ACKNOWLEDGMENT

The authors thank the funders who made this research possible. The primary sponsorship for the experimental work was provided by BRANZ (from the Building Research Levy), Te Hiranga Rū QuakeCoRE, the Natural Hazards Commission Toka Tū Ake (formerly EQC), Concrete NZ, and the University of Canterbury. Appreciation is also directed to the Advisory Group of the 'ReCast Floors' project for their guidance in shaping the test program. The program's successful completion was made possible by the technical staff at the University of Canterbury, in particular, Dave Carney, Alan Thirlwell, Russell McConchie, Norman King, Dave MacPherson, and John Maley. Additionally, many students contributed to the setup, execution and analysis of these experiments, namely Eldhose Paulose, Max Chirapattanakorn, Trevor Garrett, Abhishek Madan, Yuxin Huang, Claire Dong, Mohamed Mostafa, Ana Sarkis, Justin Brown, Jacob Nicholls and Alex Kirby.

This project was partially supported by QuakeCoRE, a New Zealand Tertiary Education Commission-funded center. This is QuakeCoRE publication number 1039.

REFERENCES

1 PCFOG (2009). *"Seismic Performance of Hollow Core Floor Systems - Guidelines for Design Assessment and Retrofit (Preliminary Draft)"*. Precast Concrete Floors Overview Group (PCFOG), Wellington, New Zealand, 163pp. http://www.nzsee.org.nz/db/PUBS/HollowCoreFloorSystems.pdf

2 DBH (2007). "*Hollowcore Floor Overview Report"*. Department of Building and Housing (DBH), Wellington, New Zealand, 21pp.

3 Standards New Zealand (1993). "NZS 3101:1982: *Code of Practice for the Design of Concrete Structures (Amendment No. 1, 2, and 3 Appended)"*. Standards New Zealand, Wellington, New Zealand, 144pp.

4 Standards New Zealand (1999). "*NZS 3101:1995: Concrete Structures Standard (Incorporating Amendment No. 1 and 2)*". Standards New Zealand, Wellington, New Zealand.

5 Iverson JK and Hawkins NM (1994). "Performance of precast/prestressed concrete building structures during Northridge earthquake". *PCI Journal*, **39**(2): 38–55. https://doi.org/10.15554/pcij.03011994.38.55

6 Norton JA, King AB, Bull DK, Chapman HE, McVerry GH, Larkin TJ and Spring KC (1994). "Northridge earthquake reconnaissance report: Report of the NZNSEE reconnaissance team on the 17 January 1994 Northridge, Los Angeles earthquake". *Bulletin of the New Zealand National Society for Earthquake Engineering*, **27**(4): 235–344. https://doi.org/10.5459/bnzsee.27.4.235-344

7 Matthews JG, Bull DK and Mander JB (2003). "Preliminary results from the testing of a precast hollowcore floor slab building". *2003 Pacific Conference on Earthquake Engineering*, Christchurch, New Zealand, 9p. https://www.nzsee.org.nz/db/2003/Print/Paper077p.pdf

8 Matthews JG (2004). *"Hollowcore Floor Slab Performance Following a Severe Earthquake"*. PhD Dissertation, University of Canterbury, Christchurch, New Zealand. http://dx.doi.org/10.26021/2247

9 Bull DK and Matthews JG (2003). "*Proof of Concept Tests for Hollowcore Floor Unit Connections"*. Research Report 2003-1, Department of Civil Engineering, University of Canterbury, 84pp. https://cdn.ymaws.com/concretenz.org.nz/resource/resmgr/docs/precast/hollowcore.pdf

10 Lindsay R (2004). *"Experiments on the Seismic Performance of Hollow-core Floor Systems in Precast Concrete Buildings"*. Masters Thesis, University of Canterbury, Christchurch, New Zealand, 340pp.

11 Trowsdale J (2004). *"Seismic Performance of Hollowcore Seating Detail Specified by Amendment No 3 NZS 3101:1995"*. Bachelors (Honours) - Final Year Project Report, University of Canterbury, Christchurch, New Zealand.

12 MacPherson C (2005). *"Seismic Performance and Forensic Analysis of a Precast Concrete Hollow-Core Floor Super-Assemblage"*. Masters Thesis, University of Canterbury, Christchurch, New Zealand, 246pp.

13 Corney SR (2018). *"Seismic Performance of Precast Concrete Flooring Systems"*. PhD Dissertation, University of Auckland, Auckland, New Zealand, 330pp. http://hdl.handle.net/2292/36862

14 Liew HY (2004). *"Performance of Hollow-core Floor Seating Connection Details"*. Masters Thesis, University of Canterbury, Christchurch, New Zealand, 155pp. https://doi.org/10.26021/14961

15 Jensen J (2006). *"The Seismic Behaviour of Existing Hollowcore Seating Connections Pre- and Post-Retrofitted"*. Masters Thesis, University of Canterbury, Christchurch, New Zealand, 292pp. http://dx.doi.org/10.26021/3244

16 Woods LJ (2008). *"The Significance of Negative Bending Moments in the Seismic Performance of Hollow-Core Flooring"*. Masters Thesis, University of Canterbury, Christchurch, New Zealand, 294pp. http://dx.doi.org/10.26021/2769

17 Standards New Zealand (2004). *"NZS 3109:1997: Concrete Construction (Incorporating Amendment No. 1 and No. 2)"*. Standards New Zealand, Wellington, New Zealand.

18 Standards New Zealand (2017). "*NZS 3101:2006: Concrete Structures Standard (Incorporating Amendment No. 1, 2 and 3)*". Standards New Zealand, Wellington, New Zealand.

19 Fenwick RC, Bull DK and Gardiner D (2010). "*Assessment of Hollow-Core Floors for Seismic Performance (Research Report 2010-02)"*. University of Canterbury, Christchurch, New Zealand, 152pp. https://ir.canterbury.ac.nz/handle/10092/4211

20 Kam WY, Pampanin S, Dhakal RP, Gavin HP and Roeder C (2010). "Seismic performance of reinforced concrete buildings in the September 2010 Darfield (Canterbury) earthquake". *Bulletin of the New Zealand Society for Earthquake Engineering*, **43**(4): 340–350. https://doi.org/10.5459/bnzsee.43.4.340-350

21 Kam WY, Pampanin S and Elwood KJ (2011). "Seismic performance of reinforced concrete buildings in the 22 February Christchurch (Lyttelton) earthquake". *Bulletin of the New Zealand Society for Earthquake Engineering*, **44**(4): 239–278. https://doi.org/10.5459/bnzsee.44.4.239-278

22 MBIE (2017). "*Investigation into the Performance of Statistics House in the 14 November 2016 Kaikōura Earthquake*". Ministry of Business and Employment (MBIE), Wellington, New Zealand. https://www.mbie.govt.nz/assets/058a9fcb92/investigation-into-the-performance-of-statistics-house.pdf

23 Henry RS, Dizhur D, Elwood KJ, Hare J and Brunsdon D (2017). "Damage to concrete buildings with precast floors during the 2016 Kaikōura earthquake". *Bulletin of the New Zealand Society for Earthquake Engineering*, **50**(2): 174–186. https://doi.org/10.5459/bnzsee.50.2.174-186

24 Mostafa MT, Hogan LS and Elwood KJ (2022). "Seismic performance of precast hollow-core floors with modern detailing: A case study". *Journal of the Structural Engineering Society New Zealand*, **35**(1): 86-100. https://www.sesoc.org.nz/download/16-seismic-performance-of-precast-hollow-core-floors-sesoc-journal-vol-35-no1-apr-2022-pdf

25 MBIE, EQC, NZSEE, SESOC and NZGS (2018). *"Technical Proposal to Revise the Engineering Assessment Guidelines - Part C5 Concrete Buildings"*. Ministry of Business Innovation and Employment (MBIE), Earthquake Commission (EQC), New Zealand Society for Earthquake Engineering (NZSEE), Structural Engineering Society (SESOC), New Zealand Geotechnical Society (NZGS), Wellington, New Zealand. https://design.resilience.nz/resources/view/c5-concrete-buildings-2018

26 Büker F (2023). "*Experimental Evaluation of the Seismic Performance of Hollow-core Floors and Retrofits*". PhD Dissertation, University of Auckland, New Zealand. https://hdl.handle.net/2292/66896

27 Corney SR, Puranam AY, Elwood KJ, Henry RS and Bull DK (2021). "Seismic performance of precast hollow-core floors: Part 1—Experimental data". *ACI Structural Journal*, **118**(5): 49–64. https://doi.org/10.14359/51732821

28 Brooke NJ, Elwood KJ, Bull DK, Liu A, Henry RS, Sullivan TJ, Hogan LS and del Rey Castillo E (2019). "Recast floors - Seismic assessment and improvement of existing precast concrete floors". *Journal of the Structural Engineering Society New Zealand*, **32**(1): 50–59.

29 Mostafa MT, Hogan LS, Stephens M and Elwood KJ (2023). "A detailed damage investigation of an instrumented ductile reinforced concrete building with precast hollow-core floors following the 2016 M-7.8 Kaikoura earthquake". *Earthquake Spectra*, **40**(3): 2179–2209. https://doi.org/10.1177/87552930231218750

30 Elwood KJ, Brooke NJ and Hogan LS (2022). "Recast Floors Project: Overview and key recommendations". *Journal of the Structural Engineering Society New Zealand*, **35**(1): 23–29. https://www.sesoc.org.nz/download/12-recast-floors-project-overview-and-key-recommendations-sesoc-journal-vol-35-no1-apr-2022-pdf

31 Mostafa MT, Büker F, Hogan LS, Elwood KJ, Bull DK and Parr M (2022). "Seismic performance of precast hollow-core units seated within the plastic hinge region". *2022 New Zealand Society for Earthquake Engineering (NZSEE) Conference*, Wellington, New Zealand, 12pp. https://repo.nzsee.org.nz/handle/nzsee/2480

32 Brooke NJ, Büker F, Bull DK, Elwood KJ, Henry RS and Hogan LS (2022). "Overview of retrofit requirements and techniques for precast concrete floors". *Journal of the Structural Engineering Society New Zealand*, **35**(1): 30–54. https://www.sesoc.org.nz/download/13-overview-of-retrofit-requirements-and-sesoc-journal-vol-35-no1-apr-2022-pdf

33 Sarkis AI, Büker F, Sullivan TJ, Elwood KJ, Brunesi E and Hogan LS (2022). "Aspects affecting the nonlinear behaviour of precast prestressed hollow-core units failing in shear". *Structural Concrete*, **23**(5): 3021–3038. https://doi.org/10.1002/suco.202100579

34 Sarkis AI, Sullivan TJ, Brunesi E and Nascimbene R (2022). "Critical modelling criteria for precast pre-stressed hollow-core slabs". *Journal of Building Engineering*, **54**: 104545. https://doi.org/10.1016/j.jobe.2022.104545

35 Parr M, Bull DK, Brooke NJ, De Francesco G, Elwood KJ, Hogan LS, Liu A and Sullivan TJ (2022). "Load-path and stiffness degradation of floor diaphragms in reinforced concrete buildings subjected to lateral loading - Part II, Data analysis". *Journal of the Structural Engineering Society New Zealand*, **35**(1): 172–203. https://www.sesoc.org.nz/download/21-part2-load-path-and-stiffness-degradation-sesoc-journal-vol-35-no1-apr-2022-pdf

36 Parr M, Büker F, De Francesco G, Bull DK, Brooke NJ, Elwood KJ, Hogan LS, Liu A and Sullivan TJ (2022). "Load-path and stiffness degradation of floor diaphragms in reinforced concrete buildings subjected to lateral loading - Part I, Experimental observations". *Journal of the Structural Engineering Society New Zealand*, **35**(1): 149–171. https://hdl.handle.net/10092/103960

37 Büker F, Brooke NJ, Hogan LS, Elwood KJ, Bull DK and Sullivan TJ (2022). "Design recommendations for strongback retrofits". *Journal of the Structural Engineering Society New Zealand*, **35**(1): 69–84. https://www.sesoc.org.nz/download/15-design-recommendations-for-strongback-sesoc-journal-vol-35-no1-apr-2022-pdf

38 Büker F, Hogan LS, Elwood KJ, Brooke NJ and Bull DK (2022). "Design recommendations for seating angle retrofits". *Journal of the Structural Engineering Society New Zealand*, **35**(1): 55–68. https://www.sesoc.org.nz/download/14-design-recommendations-for-seating-angle-sesoc-journal-vol-35-no1-apr-2022-pdf

39 Büker F, Parr M, De Francesco G, Hogan LS, Bull DK, Elwood KJ, Liu A and Sullivan TJ (2022). "Seismic damage observations of precast hollow-core floors from two full-scale super-assembly tests". *Journal of the Structural Engineering Society New Zealand*, **35**(1): 125–147. https://www.sesoc.org.nz/download/19-seismic-damage-observations-of-precast-sesoc-journal-vol-35-no1-apr-2022-pdf

40 Puranam AY, Corney SR, Elwood KJ, Henry RS and Bull DK (2021). "Seismic performance of precast hollow-core floors: Part 2-assessment of existing buildings". *ACI Structural Journal*, **118**(5): 65–77. https://doi.org/10.14359/51732822

41 Standards New Zealand (1984). "*NZS 4203:1984 - Code of Practice for General Structural Design and Design Loadings for Buildings*". Standards New Zealand, Wellington, New Zealand.

42 De Francesco G, Sullivan TJ and Nievas CI (2022). "Highlighting the need for multiple loading protocols in bi-directional testing". *Bulletin of the New Zealand Society for Earthquake Engineering*, **55**(2): 80-94. https://doi.org/10.5459/bnzsee.55.2.80-94

43 Parr M (2023). "*Retrofit Solutions for New Zealand Hollow-Core Floors and Investigation of Reliable Diaphragm Load-Paths in Earthquakes*". PhD Dissertation, University of Canterbury, Christchurch, New Zealand. http://dx.doi.org/10.26021/14176

44 Büker F, Hogan LS, Elwood KJ, Bull DK and Brooke NJ (2025). "Development and performance evaluation of seismic retrofits for precast hollow-core floors". *Earthquake Spectra (Submitted)*.

45 Büker F, Elwood KJ, Hogan LS, Parr M, de Francesco G, Bull DK and Sullivan TJ (2024). "Earthquake-induced web cracking in hollow-core floors". *18th World Conference on Earthquake Engineering*, Milan, Italy, 11pp.

46 Corney SR, Elwood KJ, Henry RS and Nims DK (2018). *"Assessment of Existing Concrete Buildings in Wellington with Precast Floors"*. Kaikoura Earthquake Research Programme (2017-18), Natural Hazards Research Platform, Lower Hutt, New Zealand, 31pp.

47 Fenwick RC and Megget LM (1993). "Elongation and load deflection characteristics of reinforced concrete members containing plastic hinges". *Bulletin of the New Zealand Society for Earthquake Engineering*, **26**(1): 28–41. https://doi.org/10.5459/bnzsee.26.1.28-41

48 Marder KJ (2018). *"Post-Earthquake Residual Capacity of Reinforced Concrete Plastic Hinges"*. PhD Dissertation, University of Auckland, Auckland, New Zealand, 272pp. http://hdl.handle.net/2292/45016

49 Sarrafzadeh MM (2021). "*Residual Capacity and Reparability of Moderately Damaged Reinforced Concrete Ductile Frame Structures*". PhD Dissertation, University of Auckland, Auckland, New Zealand, 430pp. https://hdl.handle.net/2292/59549

50 MBIE, NHC, NZSEE, SESOC and NZGS (2025). *"Non-EPB Seismic Assessment Guidelines - Part C: Concrete Buildings C5"*. Ministry of Business Innovation and Employment (MBIE), The Natural Hazards Commission Toka Tū Ake (NHC), New Zealand Society for Earthquake Engineering (NZSEE), Structural Engineering Society (SESOC), New Zealand Geotechnical Society (NZGS), Wellington, New Zealand. https://design.resilience.nz/resources/view/c5-concrete-buildings